Effects of Hydrothermal Reaction of Sulfuric Acid Lignin from *Cryptomeria japonica* for Industrial Utilization

Qiang Liu, Yasuyuki Matsushita,* Dan Aoki, Sachie Yagami, and Kazuhiko Fukushima

Sulfuric acid lignin (SAL), one of the major biorefinery industry residues from the acid saccharification process on lignocellulosic materials for bio-fuel generation, is becoming a major problem for the sustainable development of the bio-refinery industry. Meanwhile, the recalcitrant and highly complex structure of SAL makes it insoluble in water and other organic solvents, resulting in a low reactivity. This study investigated the effects of hydrothermal reactions on SAL to enhance its solubility and reactivity. A hydrothermal reaction was first conducted on SAL from *Cryptomeria japonica* to obtain a completely water-soluble lignin. Fourier transform infrared spectroscopy, gel permeation chromatography, gas chromatography, and nuclear magnetic resonance (NMR) analyses revealed that the hydrothermal reaction of the SAL caused depolymerisation, demethylation, and the introduction of phenolic hydroxyls. Furthermore, another experiment was conducted on synthesizing a lignin polymer model compound (DHP) with ^{13}C-labelled on the aromatic ring, followed by hydrothermal reaction and acetylation. Detailed structural information of DHP under hydrothermal reaction was obtained by solid-state cross polarization magic angle spinning NMR analysis. Reactivity of the hydrothermally treated SAL was enhanced by the hydrothermal reaction through the reversed increasing of the phenolic hydroxyl/aliphatic hydroxyl ratio in the condensed lignin units.

INTRODUCTION

In recent decades, the depletion of traditional fossil fuel resources and irreversible climate change attributed to anthropogenic carbon dioxide emissions have been viewed with increasing concern (Huber *et al.* 2006). This concern drives a strong global interest in carbon-neutral renewable energy sources and has promoted considerable efforts to tap into these sources (Doherty *et al.* 2011). As a result, the production of biofuel from biomass has increased remarkably. The industrial production of fuels and feedstocks from plant sources has focused on resources that can be most readily and economically processed. Depending on the type of plant sources used, such as oil palm, sugarcane, or corn (Balat *et al*. 2008), there is intensive competition for arable land with crops intended for human or animal consumption, putting increasing pressure on food prices and accelerating environmental degradation (Cotana *et al.* 2014). In contrast, the use of lignocellulosic bio-refinery processes to produce bio-fuel has enormous potential because of the abundance and renewable nature of lignocellulosic materials (Ek *et al.* 2009). Among the bio-refinery processes for lignocellulosic resources, acid hydrolysis-based saccharification of woody

materials using concentrated sulfuric acid as a catalyst is an effective method. This method is advantageous because it gives a higher yield of monosaccharides after hydrolysis, unlike enzymatic hydrolysis (Matsushita and Yasuda 2005; Matsushita *et al.* 2008).

However, the procedure also produces large quantities of sulfuric acid lignin (SAL), which shows variability in the physico-chemical properties and an extremely low reactivity, which limits its industrial uses greatly (Lora and Glasser 2002). Therefore, the development of value-added polymers and bioproducts from SAL is considered to be of utmost importance, not only to develop this acid hydrolysis-based saccharification process for achieving a sustainable economy, but also because of the increasing importance to add value to lignin produced as a bio-residue (Matsushita 2015). The solubility of residual lignin is a cornerstone of many applications and mainly depends on its chemical structure, molecular weight (*M*) distribution, and the presence of hydrophilic moieties in the lignin molecule (Shukry *et al.* 2008).

The solubility of lignin in various organic solvents has been thoroughly studied (Cybulska *et al.* 2012; Sameni *et al.* 2017). However, there is still a lack of information on lignin solubility in water. The use of water as a medium could greatly expand the potential uses of lignin.

Sulfuric acid lignin has been identified to have a highly condensed structure derived from intermolecular dehydrative condensation reactions between benzylic carbons and aromatic nuclei (Yasuda *et al.* 1983). Further studies have revealed that the condensed aromatic nuclei of SAL could be selectively exchanged with phenol in the presence of sulfuric acid as a catalyst (Yasuda *et al.* 1998). Phenolization has been characterized as the key step for converting SAL into water-soluble lignin with phenol in the presence of a sulfuric acid catalyst.

It was also found that the reactivity of phenolized sulfuric acid lignin (P-SAL) is enhanced by phenolization, resulting in its depolymerization and the introduction of a reactive *p*-hydroxyphenyl moiety to the side chain α-position instead of condensed-type aromatic nuclei (Yasuda *et al.* 1998). However, this conversion system has resulted in a huge environmental burden and high production costs, which have necessitated the urgent development of a simplified method.

Further investigation by Matsushita *et al.* (2009) indicated that hydrothermal reactions, which avoid using phenol to promote phenolization, can also convert SAL into a water-soluble polymer and provide an effective way for simplifying the conversion system to obtain engineering products. This finding is inspiring because the solubilization of lignin is especially important for converting technical lignin for industrial utilization. Nevertheless, few studies have suggested a mechanism for the hydrothermal reaction of SAL. Knowledge of the hydrothermal reaction of SAL may provide useful information for the further improvement of acid-catalyzed saccharification.

To understand the underlying mechanism of the hydrothermal reaction of SAL, more detailed information about the characteristics and functions of SAL was gathered by Fourier transform infrared (FT-IR) spectroscopy, gas chromatography-flame ionization detection (GC-FID), solid-state and liquid nuclear magnetic resonance (NMR), and elemental analyses. Also, the enzymatic dehydrogenative polymer (DHP), which is a polymer model of lignin, was investigated to gain a better understanding of the structural changes that occur during the hydrothermal reaction. Furthermore, another experiment on synthesizing DHP was conducted with ^{13}C-labelling on the aromatic ring, followed by hydrothermal reaction and acetylation. The detailed structural information of the DHP after

hydrothermal reaction was obtained by solid-state cross polarization magic angle spinning (CP/MAS)-NMR analysis.

EXPERIMENTAL

Preparation of the SAL

Japanese cedar (*Cryptomeria japonica*) was used as the study material. Its chips were ground into a powder, and powder particles 60 to 80 mesh in size were selected for the study. The Japanese cedar powder first had its extractives removed by introducing it to a Soxhlet extractor system (Based on TAPPI method 204, Tokyo, Japan, Kiriyama Led.) (Benzene/ethanol = 2:1). The SAL was prepared from this extracted powder by hydrolysis using sulfuric acid with the following process (Yasuda and Ota 1987; Matsushita *et al.* 2004). Sulfuric acid (72 wt.%; 30.5 mL) was added to 12.5 g of wood powder and stirred at room temperature for 30 min. Then, 70 mL of water were added and the system was allowed to react at 90 °C for 90 min. The reaction products were washed with water using a centrifuge until the cleaning fluid was neutral and then filtered using a glass filter. The residue was dried at 105 °C to obtain the SAL (4.40 g; yield was calculated as 35.2 wt.% based on the wood powder).

Hydrothermal Reaction of the SAL with Alkali

The hydrothermal reaction was conducted as follows. A mixture containing 100 mg of SAL, 100 mg of alkali (NaOH), and 3 mL of water was sealed in a stainless-steel tube with an inner volume of 12 cm^3 and heated at the required temperature (250 °C, 275 °C, and 300 °C) for the desired length of time (2 h, 4 h, and 6 h). After the reaction, the stainless-steel tube was cooled immediately to room temperature by immersion in a water bath. The reaction mixture was filtered using a 1G3 filter (Sekiya, Tokyo, Japan) to obtain the liquid form of the hydrothermally treated SAL (HSAL). The liquid form of the hydrothermally treated SAL was collected carefully and dialyzed using a cellulose tube with a 3500 molecular weight cutoff (Tubing TM 3500; BioDesign, Carmel, NY, USA) to remove inorganic reagents. The reaction products were lyophilized to obtain the hydrothermally treated SAL (HSAL) (Yasuda *et al*. 1998; Matsushita *et al.* 2011).

Determination of the Methoxy Group Content of the HSALs

According to a previous study (Sumerskii *et al*. 2017), the methoxy group content was determined in the following manner. Three milligrams of HSALs and 10 mL of hydroiodic acid (57%, w/w) were sealed in a glass vial and heated at 130 °C for 20 min. After cooling in an ice bath, 1 mL of a standard solution (62.5 μL of ethyl iodide dissolved in tetrachloromethane solution) was added through the septum. The vial was opened, and then the reaction mixture was extracted with 10 mL of tetrachloromethane, which was followed by the addition of sodium sulfate to remove the extra water in the tetrachloromethane layer. The methyl iodide content was determined by GC-FID (GC-353; GL Sciences, Tokyo, Japan) with a TC-1 capillary column (60 m × 0.25 mm i.d.; GL Sciences) at an injection temperature of 200 °C, detector temperature of 230 °C, and column temperature of 40 °C to 280 °C (temperature program: held at 40 °C for 5 min and increased to 280 °C at a rate of 10 °C/min) with a N$_2$ carrier flow rate of 1.1 mL/min.

Molecular Weight Distribution

The *M* distribution was measured with gel permeation chromatography on a Sepharose CL-6B (51 cm × 1.8 cm; GE Healthcare, Uppsala, Sweden) with 0.5 N NaOH as the eluent and an ultraviolet detector (280 nm). Sodium polystyrene sulfonates (*M* values of 1800 g/mol, 5400 g/mol, 18000 g/mol, and 100000 g/mol) were used as the standards (González *et al.* 2000).

FT-IR Spectroscopy

The analysis of different lignin samples was performed with FT-IR spectroscopy (8400s, SHIMADZU, Kyoto, Japan). The region between 4000 cm^{-1} and 400 cm^{-1} was recorded, with a resolution of 4 cm^{-1} and 32 scans. Each sample was prepared according to the potassium bromide method (Winder and Goodacre 2004).

Acetylation of the Lignin

In order to improve the solubility in NMR organic solution (chloroform-d) for enabling subsequent NMR analysis, acetylation of lignin was applied here. The lignin samples (acid-washed HSAL 250-2 and commercial kraft lignin, dried under vacuum at 40 °C for 8 h to 16 h) were acetylated with acetic anhydride/pyridine (1:1, v/v) in a 50-mL round-bottom flask at room temperature for 24 h (Olarte 2011). The lignin concentration in this solution was approximately 50 mg/mL. After 24 h, the solution was diluted with 30 mL of ice water. The residue was then dissolved in chloroform and washed twice with filtered deionized water through a membrane filter (H050A047A, ADVANTEC, Tokyo, Japan) and the product was collected as a precipitate. The precipitate was dried under high vacuum at 40 °C for 24 h.

NMR Analysis of the SAL

The ^{1}H/^{13}C-NMR spectra were recorded with a Bruker AVANCE 400 MHz spectrometer (Hitachi, Tokyo, Japan) using chloroform-D as the solvent (Mahmood *et al.* 2015). Chemical shifts were presented in parts per million using tetramethylsilane (0 ppm) as the internal standard.

^{13}C-labelled DHP Synthesis

Based on a previous study (Matsushita *et al.* 2009), ^{13}C-labelled DHP was synthesized as follows. Figure 1 shows that 90% vanillin and 10% ^{13}C-labelled vanillin (phenyl-^{13}C6, Sigma-Aldrich) were the original materials and were reacted with monoethyl-malonate to obtain (E)-Ethyl ferulate.

Solid-state ^{13}C CP/MAS NMR of the AHS-DHP

The CP/MAS ^{13}C-NMR spectra were recorded on a JEOL ECA-700 (JEOL, Ltd., Tokyo, Japan) system. The solid samples were pressed into 7-mm zirconia rotors and spun at a ^{13}C resonance frequency of 175 MHz, scan number of 17000, and MAS of 15 kHz (Nakazawa and Asakura 2002).
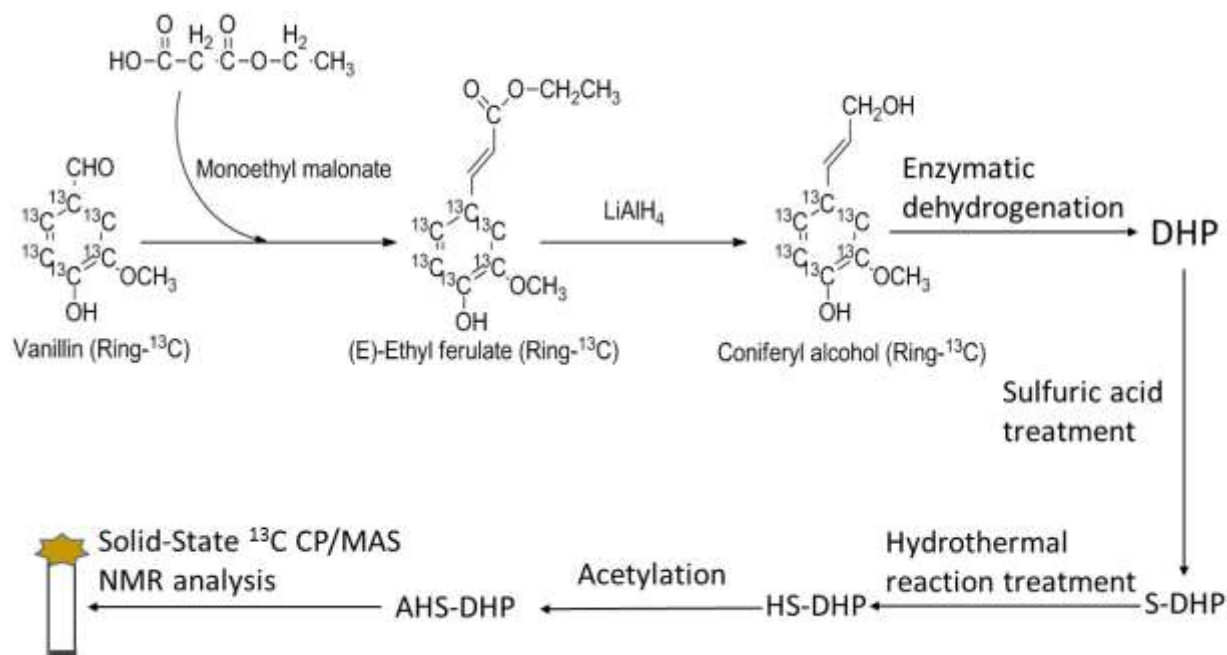
Fig. 1. Schematic diagram of the ^{13}C-labelled DHP experiment

RESULTS AND DISCUSSION

Solubility Properties of the HSALs

The dissolvability experiments (Tables 1 and S1) revealed that the hydrothermal reaction could convert SAL into water-soluble compounds in neutral water. However, the HSAL did not dissolve in the organic solvents (low polarity).

According to a previous report by Sameni *et al.* (2017), lignin is insoluble in most organic solvents mainly because of a noticeable difference between the HSALs and solvents. Surprisingly, the HSAL completely dissolved in water. Because a direct correlation was determined, increasing the number of OH groups in the C9-formula was noted to increase the solubility of lignin in water. The higher solubility of lignin in water might have been because of the introduction of hydrophilic groups during the hydrothermal reaction.

Table 1. Results of the Dissolvability Experiment

Sample	Hexane	Chloroform	Ethyl Acetate	THF	Acetone	Methanol	H$_2$O	0.1 M NaOH	Pyridine
SAL	×	×	×	×	×	×	×	×	×
HSAL	×	×	×	×	×	Δ	○	○	×
HSAL-aw	×	×	×	Δ	Δ	Δ	×	○	○

Note: HSAL-aw: hydrothermal reacted sulfuric acid lignin with acid washing; ○: completely dissolved; Δ: partially dissolved; ×: completely insoluble

Molecular Weight Distribution

Gel permeation chromatography was performed to obtain the weight-average molecules weight M_w under various reaction conditions. The results are shown in Table 2. The M_w value of the HSALs gradually decreased from 1.76×10^4 g/mol to 6.5×10^3 g/mol as the hydrothermal reaction temperature was increased from 200 °C to 300 °C (HSAL 200-2, HSAL 225-2, HSAL 250-2, HSAL 275-2, and HSAL 300-2).

Table 2. Molecular Weight Distributions of the HSALs

Sample	Temperature (°C)	Time (min)	Mw (×10³ g/mol)
HSAL 250-1	250	60	7.5
HSAL 250-2	250	120	7.3
HSAL 250-3	250	180	5.8
HSAL 250-4	250	240	5.0
HSAL 250-6	250	360	4.1
HSAL 200-2	200	120	17.6
HSAL 225-2	225	120	7.9
HSAL 275-2	275	120	7.2
HSAL 300-2	300	120	6.5

Heating rate = 50 °C/min (GC-oven box)

The M_w values of the HSALs decreased, which prolonged the hydrothermal reaction (HSAL 250-1, HSAL 250-2, HSAL 250-3, HSAL 250-4, and HSAL 250-6). Hence, better depolymerization conditions for the HSALs appeared to extend the reaction time at a specific temperature. Additionally, after the hydrothermal reaction conditions were transformed into H-factors (Table S1), the M_w of HSAL 300-2 (H-factor: 7081405) was 6.5×10^3 g/mol under the highest H-factor. This result was higher than the M_w of HSAL 250-6 (Mw: 4.1×10^3 g/mol, H-factor: 1440114). The reason for this might have been the unavoidable condensation reaction that occurred during the harsher hydrothermal reaction. Other researchers have reported similar results (Mahmood *et al.* 2014).

Methoxy Group Content of the SAL and HSALs

The results of the methoxy group analysis of the SAL and HSALs by GC-FID are summarized in Fig. 2. The observed change in the methoxy content of the SAL indicated that demethylation occurred during the hydrothermal reaction. In the first group of HSALs, which reacted at the same temperature and an increasing reaction time, a slow decrease in the speed with the time was observed. Meanwhile, demethylation was well facilitated by increasing the hydrothermal reaction temperature. A decreased ratio of 85.5% was seen after demethylation at 300 °C for 2 h. After the hydrothermal reaction conditions were transformed into H-factors (Table S1), the higher H-factor was attributed to demethoxylation.
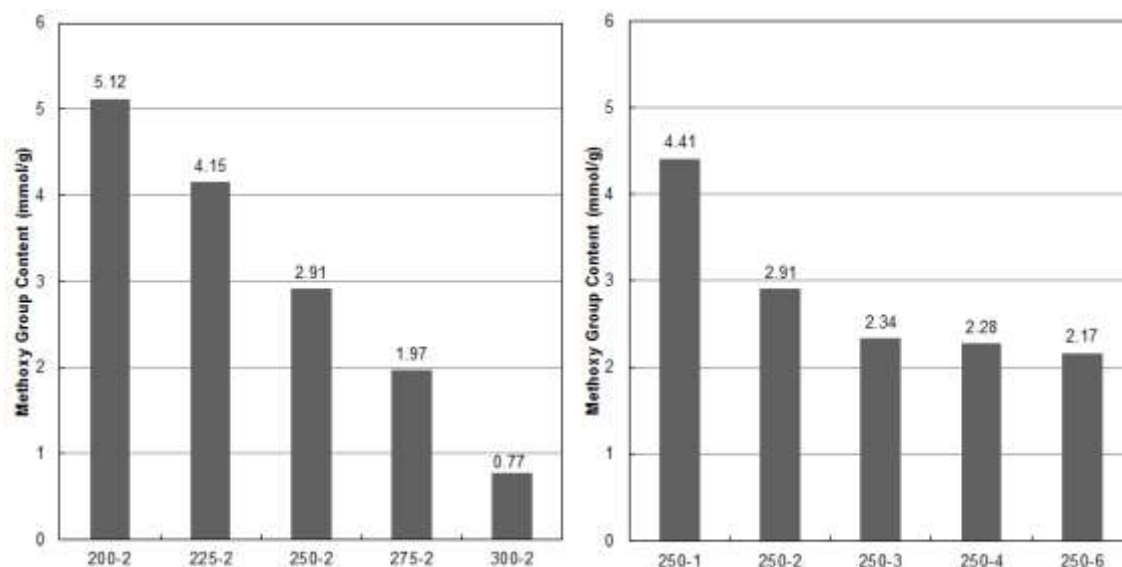
Fig. 2. Comparison of the methoxy group content of the HSALs

Elemental Analysis

Table 3 presents the elemental analysis results of the HSALs. The SAL had an elemental composition (on a dry basis) of 63.33 wt.% carbon, 5.65 wt.% hydrogen, and 30.87 wt.% oxygen. Conversely, HSAL 250-6 had an elemental composition (on a dry basis) of 61.14 wt.% carbon, 3.96 wt.% hydrogen, and 34.77 wt.% oxygen. The comparison of the oxygen contents of the SAL and HSALs indicated that the oxygen content increased during the hydrothermal reaction. This result was consistent with the comparison results of the commercial alkali soluble lignin and insoluble lignin. Additionally, an increase in the oxygen content was observed under harsher hydrothermal reaction conditions. This suggested that hydrophilic groups, such as hydroxyls, were introduced by the hydrothermal reaction.

Table 3. Elemental Analysis of the SAL/HSALs

Sample	Temperature (°C)	Time (min)	C (%)	H (%)	O (%)
HSAL 250-1	250	60	63.18	4.64	32.03
HSAL 250-3	250	180	61.89	3.77	34.22
HSAL 250-6	250	360	61.14	3.96	34.77
HSAL 200-2	200	120	62.56	5.01	32.31
HSAL 225-2	225	120	62.3	4.67	32.91
HSAL 275-2	275	120	62.15	3.79	33.86
HSAL 300-2	300	120	61.54	3.57	34.74
Alkali Lignin (Insoluble in water)			62.42	5.85	31.03
Alkali Lignin (Soluble in water)			49.7	4.75	45.42
SAL			63.33	5.65	30.87

Analysis of the FT-IR Spectra

The FT-IR spectra of the SAL and HSALs are shown in Fig. 3. The typical absorptions at 1605 cm^{-1}, 1512 cm^{-1}, and 1427 cm^{-1} were derived from the aromatic skeletal vibrations of lignin, which indicated that the lignin aromaticity was not severely disrupted during the hydrothermal reaction (Samuel *et al.* 2013).
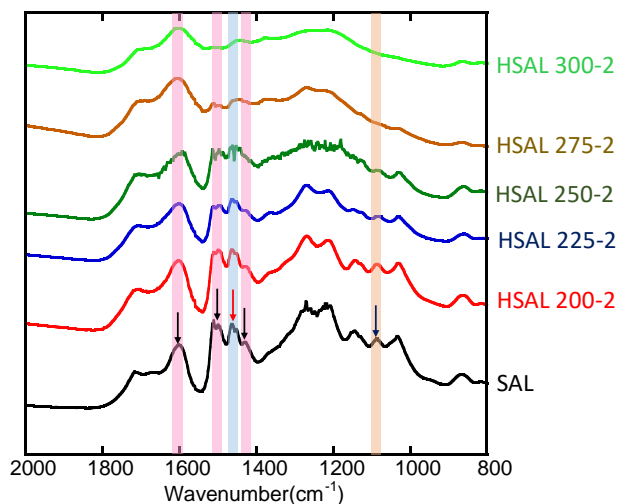
Fig. 3. FT-IR spectra of the SAL and HSALs

The intensity of the absorbance at 1465 cm^{-1} (C–H deformation of –CH$_2$– and –CH$_3$ groups) decreased from the SAL to HSALs, which suggested that the methoxy group content decreased with an increasing severity of the hydrothermal reaction conditions as a result of demethylation (Wen *et al.* 2013). The absorption at 1265 cm^{-1} (C-O vibration of the guaiacyl (G) ring) in the HSALs also presented a lower intensity than that of the SAL. This might have been related to the demethylation of the SAL under the harsh hydrothermal conditions, which led to a decrease in the amount of G-type lignin units and phenolic hydroxyl group content (Winder and Goodacre 2004). The peak at 1000 cm^{-1} to 1100 cm^{-1} was derived from ether linkages, which decreased with an increase in the hydrothermal reaction temperature from 200 °C to 300 °C. This indicated ether linkages cleaved during the hydrothermal reaction (Sun *et al.* 2013). This result was also supported by the NMR findings. Additionally, it was observed that the intensity of the peak at 1705 cm^{-1} (C=O stretching in the conjugated ketone and carbonyl groups) remarkably increased with the severity of the hydrothermal reaction (Leschinsky *et al.* 2008a,b).

^{1}H NMR Spectra of the Acetylated SAL

According to the solubility test on the HSAL, it was found that the HSAL did not dissolve in the organic solvents, which made it difficult to perform the NMR analysis directly. Meanwhile, acetylating the lignin results in a better solubility in organic solvents (Olarte 2011) and therefore was applied here to further investigate the functional groups of the obtained HSALs by liquid-state ^{1}H NMR. The ^{1}H NMR spectrum of HSAL 250-2 is shown in Fig. 4A. The sample was acetylated to convert the hydroxyl groups into acetyl groups before the ^{1}H NMR spectra were recorded. The number of acetyl groups in the acetylated HSAL was calculated by the sum of aliphatic and phenolic groups in the expanded C9 formula (Mahmood *et al.* 2014).

The spectra of the phenolic (2.2 ppm to 2.6 ppm) and aliphatic acetates (1.6 ppm to 2.2 ppm) were superimposed onto each other (Mahmood *et al.* 2015). Quantification of the aliphatic and phenolic hydroxyls was done by peak integration in comparison with dibromomethane internal standard peaks (4.9 ppm). The HSAL had a total hydroxyl amount of 5.7 mmol/g.

The deconvoluted spectrum (Fig. 4B) of the acetylated spectrum (Fig. 4A), which was based on the integral sum of the Lorentz distribution, showed that the fraction ratio of the phenolic (phenolic-OH) and aliphatic acetates (aliphatic-OH) was 5.1:1. This suggested that the aliphatic-OH groups were oxidized and modified gradually during the hydrothermal reaction. Similar results for milled SAL extracted from Japanese red pine were reported by Yasuda *et al.* (1983).

Additionally, Table 4 shows that the phenolic hydroxyl content in the HSAL (4.77 mmol/g) was notably increased compared with that in the softwood Bjorkman lignin (L; 1.26 mmol/g), milled softwood Bjorkman lignin (ML; 1.32 mmol/g), and milled SAL (MSAL; 2.29 mmol/g).
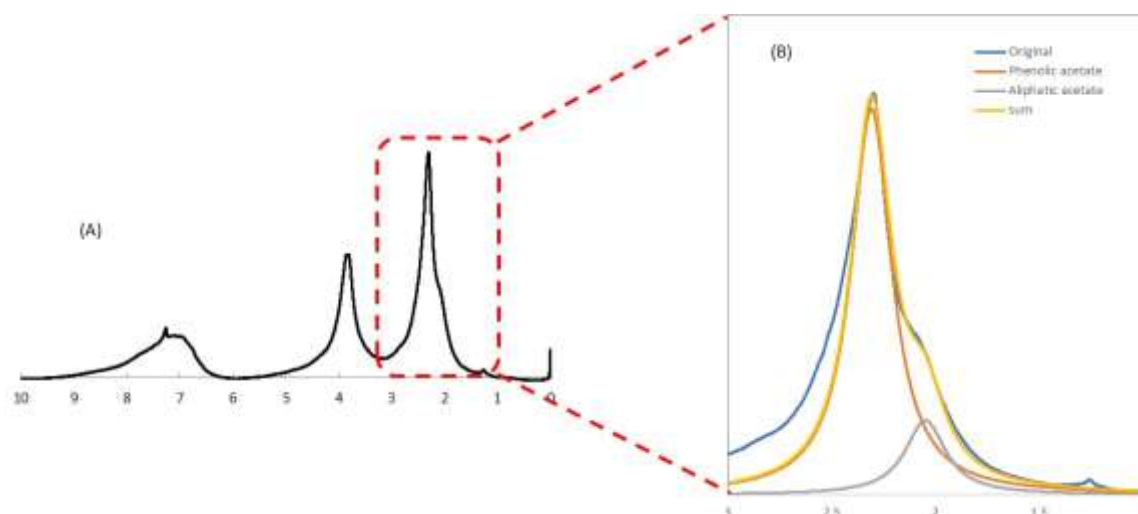
Fig. 4. NMR spectrum of the acetylated HSAL 250-2 (A) and the deconvoluted spectrum (B) of the acetylated HSAL 250-2 spectrum based on the integral sum of the Lorentz distribution

Table 4. Properties of the Lignin Preparations

Sample	OH (%)		Total	Ratio of Ph-OH/Al-OH
	Phenolic-OH	Alcoholic-OH		
L	1.26	8.84	10.1	0.14
ML	1.32	8.58	9.9	0.15
MSAL	2.29	6.91	9.2	0.33
HSAL	4.77	0.93	5.7	5.14

L: softwood Bjorkman lignin; ML: milled softwood Bjorkman lignin; and MSAL: milled sulfuric acid lignin (Yasuda *et al.* 1983)

The increase in the phenolic hydroxyl content was mainly related to the cleavage of aryl ether linkages during the hydrothermal reaction and the introduction of phenolic hydroxyls. Meanwhile, the total hydroxyl group content in the L (10.1 mmol/g) was higher than that in the HSAL (5.7 mmol/g). This reduction was mainly caused by the decrease in the aliphatic hydroxyl content, which was related to the condensation reaction that occurred during the hydrothermal reaction. The observed increase in the phenolic hydroxyl content in the condensed lignin units was also confirmed by the solid-state ^{13}C CP/MAS NMR analysis of the acetylated HSAL.

^{13}C CP/MAS NMR Spectral Analysis

The HSAL solubility in the NMR organic solvent was low, which made it difficult to obtain a clear ^{13}C-NMR spectrum of the HSAL, even after acetylation. Therefore, DHP was sequentially subjected to sulfuric acid treatment, hydrothermal reaction (280 °C and 2 h), and acetylation to convert the DHP into AHS-DHP.

The solid-state ^{13}C CP/MAS NMR analysis of the AHS-DHP with ^{13}C-labelled on the aromatic ring, as a model of the HSAL, was performed to obtain detailed information about the benzene ring and spectra. This analysis is shown in Fig. 5. The peak at 100 ppm to 160 ppm was assigned to the aromatic region. The sharp peak observed at 155 ppm signified an aromatic carbon connected with oxygen, which indicated an increase in the phenolic hydroxyl content during the hydrothermal reaction. Except for a portion of the spinning side band (red spectrum in Fig. 5), the remaining part of the peaks in the range of 30 ppm to 60 ppm illustrated a high degree of aromatic ring cracking, which contributed to the formation of degraded groups from the aromatic ring during the hydrothermal reaction.
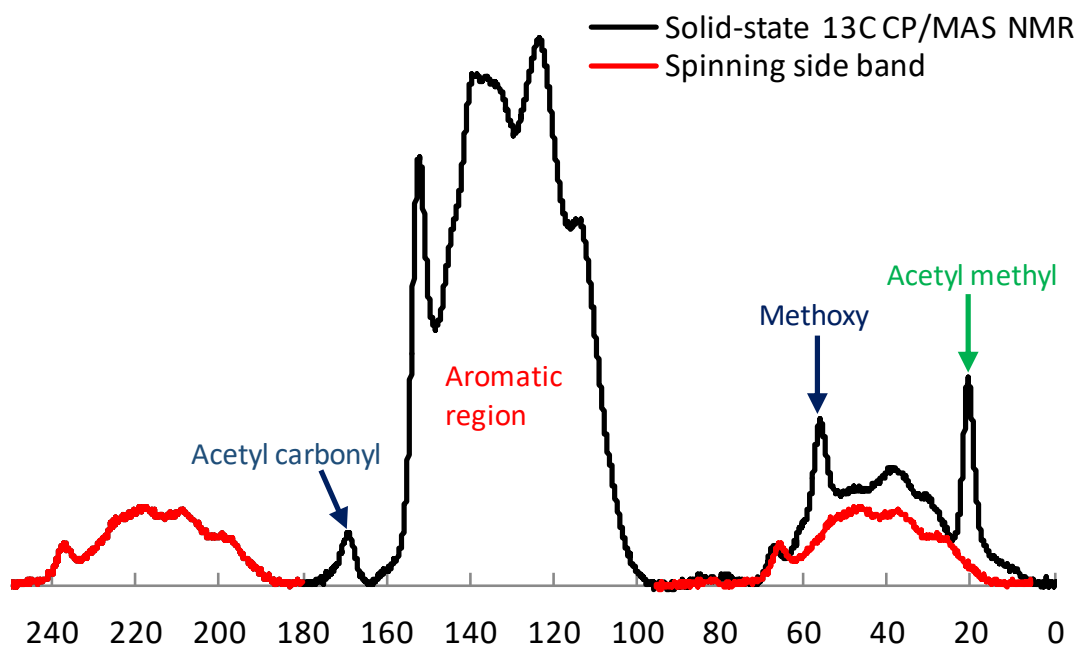
Fig. 5. Solid-state ^{13}C CP/MAS NMR spectra of the AHS-DHP

CONCLUSIONS

1. The hydrothermal reaction can convert sulfuric acid lignin (SAL) into a soluble lignin in neutral water and an insoluble lignin in organic solvents. The reason for the higher solubility of lignin in water might have been the introduction of hydrophilic groups by demethylation during the hydrothermal reaction.

2. After transforming the hydrothermal reaction conditions into H-factors (Table S1), it was suggested that the higher H-factor could have been because of demethoxylation. However, this positive correlation was not obtained for the molecular weight of the HSALs. The reason for this might have been the unavoidable condensation reaction during the harsher hydrothermal reaction.

3. The ^{1}H NMR spectrum of the HSAL illustrated that the phenolic hydroxyl content in the HSAL (4.77 mmol/g) was noticeably increased compared with that of original industrial lignins (1.26 mmol/g to 2.29 mmol/g) and the ratio of the phenolic-OH/aliphatic-OH was reversed, from 0.33 (MSAL) to 5.14 (HSAL). Those results were also confirmed by the results of the elemental analysis and FT-IR spectra.

4. Furthermore, the solid-state CP/MAS-NMR analysis of the ^{13}C-labelled AHS-DHP indicated that the HSAL reactivity was enhanced by the hydrothermal reaction because the reversal increased the phenolic hydroxyl content and portion of aromatic ring cracking during the hydrothermal reaction.

5. Based on this information, it was suggested that demethylation, depolymerisation, the introduction of phenolic hydroxyls, and condensation reactions of lignin occurred simultaneously during the hydrothermal reaction. In view of mass industrial utilization, hydrothermal conversion has revealed new insights for readily and economically converting SAL into water-soluble polymers, which will greatly increase the potential of its further industrial utilization.

ACKNOWLEDGMENTS

REFERENCES CITED

Balat, M., Balat, H., and Öz, C. (2008). "Progress in bioethanol processing," *Prog. Energ. Combust.* 34(5), 551-573. DOI: 10.1016/j.pecs.2007.11.001

Cotana, F., Cavalaglio, G., Nicolini, A., Gelosia, M., Coccia, V., Petrozzi, A., and Brinchi, L. (2014). "Lignin as co-product of second generation bioethanol production from ligno-cellulosic biomass," *Enrgy. Proced.* 45, 52-60. DOI: 10.1016/j.egypro.2014.01.007

Cybulska, I., Brudecki, G., Rosentrater, K., Julson, J. L., and Lei, H. (2012). "Comparative study of organosolv lignin extracted from prairie cordgrass, switchgrass and corn stover," *Bioresource Technol.* 118, 30-36. DOI: 10.1016/j.biortech.2012.05.073

Doherty, W. O. S., Mousavioun, P., and Fellows, C. M. (2011). "Value-adding to cellulosic ethanol: Lignin polymers," *Ind. Crop. Prod.* 33(2), 259-276. DOI: 10.1016/j.indcrop.2010.10.022

Ek, M., Gellerstedt, G., and Henriksson, G. (2009). *Pulp and Paper Chemistry and Technology: Volume 1 - Wood Chemistry and Biotechnology*, De Gruyter, Boston, MA.

González, A. M., Salager, J. L., Brunetto, M. R., Gallignani, M., Burguera, J. L., Burguera, M., and Petit de Peña, Y. (2000). "Determination of molecular weight distribution of lignin derivatives by aqueous phase high performance size exclusion chromatography (HPSEC)," *J. High Res. Chromatog.* 23(12), 693-696. DOI: 10.1002/1521-4168(20001201)23:12<693::AID-JHRC693>3.0.CO;2-T

Huber, G. W., Iborra, S., and Corma, A. (2006). "Synthesis of transportation fuels from biomass: Chemistry, catalysts, and engineering," *Chem. Rev.* 106(9), 4044-4098. DOI: 10.1021/cr068360d

Leschinsky, M., Zuckerstätter, G., Weber, H. K., Patt, R., and Sixta, H. (2008a). "Effect of autohydrolysis of *Eucalyptus globulus* wood on lignin structure. Part 1: Comparison of different lignin fractions formed during water prehydrolysis," *Holzforschung* 62(6), 645-652. DOI: 10.1515/HF.2008.117

Leschinsky, M., Zuckerstätter, G., Weber, H. K., Patt, R., and Sixta, H. (2008b). "Effect of autohydrolysis of *Eucalyptus globulus* wood on lignin structure. Part 2: Influence of autohydrolysis intensity," *Holzforschung* 62(6), 653-658. DOI: 10.1515/HF.2008.133

Lora, J. H., and Glasser, W. G. (2002). "Recent industrial applications of lignin: A sustainable alternative to nonrenewable materials," *J. Polym. Environ.* 10(1-2), 39-48. DOI: 10.1023/a:1021070006895

Mahmood, N., Yuan, Z., Schmidt, J., and Xu, C. C. (2014). "Production of polyols *via* direct hydrolysis of kraft lignin: Optimization of process parameters," *Journal of Science and Technology for Forest Products and Processes* 4(2), 44-51.

Mahmood, N., Yuan, Z., Schmidt, J., and Xu, C. C. (2015). "Hydrolytic depolymerization of hydrolysis lignin: Effects of catalysts and solvents," *Bioresource Technol.* 190, 416-419. DOI: 10.1016/j.biortech.2015.04.074

Matsushita, Y. (2015). "Conversion of technical lignins to functional materials with retained polymeric properties," *J. Wood Sci.* 61(3), 230-250. DOI: 10.1007/s10086-015-1470-2

Matsushita, Y., Imai, M., Iwatsuki, A., and Fukushima, K. (2008). "The relationship between surface tension and the industrial performance of water-soluble polymers prepared from acid hydrolysis lignin, a saccharification by-product from woody materials," *Bioresource Technol.* 99(8), 3024-3028. DOI: 10.1016/j.biortech.2007.06.015

Matsushita, Y., Inomata, T., Takagi, Y., Hasegawa, T., and Fukushima, K. (2011). "Conversion of sulfuric acid lignin generated during bioethanol production from lignocellulosic materials into polyesters with ε-caprolactone," *J. Wood Sci.* 57(3), 214-218. DOI: 10.1007/s10086-010-1158-6

Matsushita, Y., Iwatsuki, A., and Yasuda, S. (2004). "Application of cationic polymer prepared from sulfuric acid lignin as a retention aid for usual rosin sizes to neutral papermaking," *J. Wood Sci.* 50(6), 540-544. DOI: 10.1007/s10086-003-0602-2

Matsushita, Y., Sekiguchi, T., Ichino, R., and Fukushima, K. (2009). "Electropolymerization of coniferyl alcohol," *J. Wood Sci.* 55(5), 344-349. DOI: 10.1007/s10086-009-1037-1

Matsushita, Y., and Yasuda, S. (2005). "Preparation and evaluation of lignosulfonates as a dispersant for gypsum paste from acid hydrolysis lignin," *Bioresource Technol.* 96(4), 465-470. DOI: 10.1016/j.biortech.2004.05.023

Nakazawa, Y., and Asakura, T. (2002). "High-resolution ^{13}C CP/MAS NMR study on structure and structural transition of *Antheraea pernyi* silk fibroin containing poly(L-alanine) and gly-rich regions," *Macromolecules* 35(6), 2393-2400. DOI: 10.1021/ma011999t

Olarte, M. V. (2011). *Base-catalyzed Depolymerization of Lignin and Hydrodeoxygenation of Lignin Model Compounds for Alternative Fuel Production*, Ph.D. Dissertation, Georgia Institute of Technology, Atlanta, Georgia.

Sameni, J., Krigstin, S., and Sain, M. (2017). "Solubility of lignin and acetylated lignin in organic solvents," *BioResources* 12(1), 1548-1565. DOI: 10.15376/biores.12.1.1548-1565

Samuel, R., Cao, S., Das, B. K., Hu, F., Pu, Y., and Ragauskas, A. J. (2013). "Investigation of the fate of poplar lignin during autohydrolysis pretreatment to understand the biomass recalcitrance," *RSC Adv.* 3(16), 5305-5309. DOI: 10.1039/C3RA40578H

Shukry, N., Fadel, S. M., Agblevor, F. A., and El-Kalyoubi, S. F. (2008). "Some physical properties of acetosolv lignins from bagasse," *J. Appl. Polym. Sci.* 109(1), 434-444. DOI: 10.1002/app.28059

Sumerskii, I., Zweckmair, T., Hettegger, H., Zinovyev, G., Bacher, M., Rosenau, T., and Potthast, A. (2017). "A fast track for the accurate determination of methoxyl and ethoxyl groups in lignin," *RSC Adv.* 7(37), 22974-22982. DOI: 10.1039/C7RA00690J

Sun, Y., Qiu, X., and Liu, Y. (2013). "Chemical reactivity of alkali lignin modified with laccase," *Biomass Bioenerg.* 55, 198-204. DOI: 10.1016/j.biombioe.2013.02.006

Wen, J.-L., Sun, S.-N., Yuan, T.-Q., Xu, F., and Sun, R.-C. (2013). "Fractionation of bamboo culms by autohydrolysis, organosolv delignification and extended delignification: Understanding the fundamental chemistry of the lignin during the integrated process," *Bioresource Technol.* 150, 278-286. DOI: 10.1016/j.biortech.2013.10.015

Winder, C. L., and Goodacre, R. (2004). "Comparison of diffuse-reflectance absorbance and attenuated total reflectance FT-IR for the discrimination of bacteria," *Analyst* 129(11), 1118-1122. DOI: 10.1039/B408169B

Yasuda, S., Hamaguchi, E., Matsushita, Y., Goto, H., and Imai, T. (1998). "Ready chemical conversion of acid hydrolysis lignin into water-soluble lignosulfonate II: Hydroxymethylation and subsequent sulfonation of phenolized lignin model compounds," *J. Wood Sci.* 44(2), 116-124. DOI: 10.1007/BF00526256

Yasuda, S., and Ota, K. (1987). "Chemical structures of sulfuric acid lignin," *Holzforschung* 41(1), 59-65. DOI: 10.1515/hfsg.1987.41.1.59

Yasuda, S., Terashima, N., and Hamanaka, A. (1983). "Chemical structure of sulfuric acid lignin. VI. Physical and chemical properties of sulfuric acid lignin," *Mokuzai Gakkaishi* 29(11), 795-800.

APPENDIX

Supplementary Material

Hydrothermal reaction

Wood powder (Japanese Cedar)

i) Soxhlet extractor system
ii) Klason lignin method

SAL

i) Hydrothermal reaction
ii) Dialyzed in a cellulose tube
iii) Freeze-dried

HSAL

NaOH solution (0.8 mol/L, m/m=1:1)
Sulfuric acid lignin (SAL)
Heated at required temperature (200, 225, 250, 275 and 300°C) for settled time (1, 2, 3, 4 and 6h)
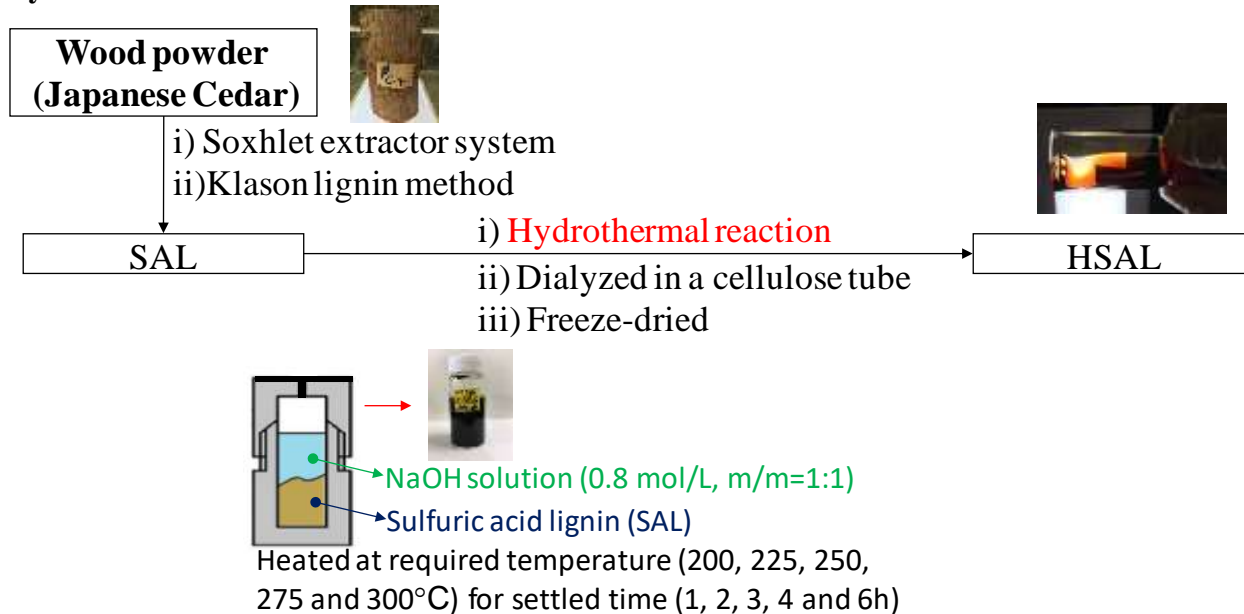
Table S1. Hydrothermal Reaction Conditions on SALs

Condition	Dosage of NaOH (mg)	Temperature (℃)	Time (min)	H-factor[a]
#250-1	100	250	60	241330
#250-2	100	250	120	481087
#250-3	100	250	180	720843
#250-4	100	250	240	960600
#250-6	100	250	360	1440114
#200-2	100	200	120	18515
#225-2	100	225	120	102198
#275-2	100	275	120	1957962
#300-2	100	300	120	7081405

[a] H-factor, $H=\int_0^t e(43.2 - \frac{16117}{T})dt$; where T=Reaction temperature and t=Reaction time; Heated rate as 50/min (GC-Oven box)

GPC

The molecular weight distribution was measured using Sepharose CL-6B(51×1.8cm) with 0.5 M NaOH aqueous solution as the eluent and ultraviolet (UV) detection (280 nm). Sodium polystyrene sulfonates (M_w=1.8×10^3 to 1.0×10^5) were used as a standard.

NMR (^{1}H-NMR, ^{13}C-NMR, ^{31}P-NMR, solid-NMR)

^{1}H/^{13}C-NMR spectra were recorded with a Bruker AVANCE 400 MHz Spectrometer (Bruker) using Pyridine-d5 as the solvent. Chemical shifts were presented in ppm downfield using TMS (tetramethyl silane, 0 ppm) as an internal standard.

Solubility Properties of HSALs

Table S2. Results of Dissolvability Experiment

Samples	Hexane	Chloroform	Ethyl Acetate	THF	Acetone	Methanol	H$_2$O	0.1 M NaOH	Pyridine
SAL	×	×	×	×	×	×	×	×	×
HSAL	×	×	×	×	×	Δ	○	○	×
HSAL-aw	×	×	×	Δ	Δ	Δ	×	○	○
Dissolvability comparison									

Note:

○：Completely dissolved

Δ：Partially dissolved

×：Completely insoluble

DHP Synthesis：
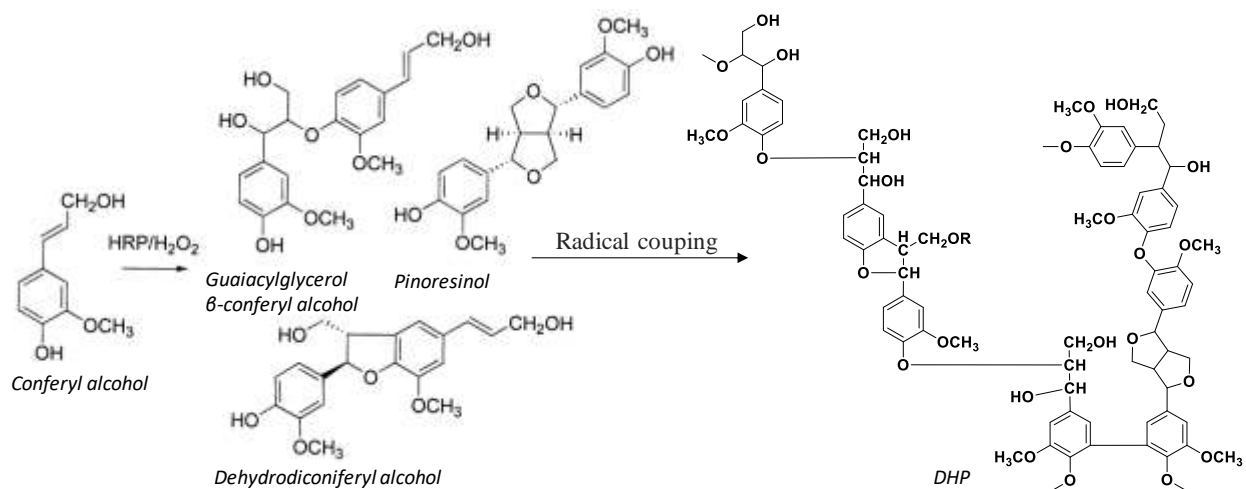
Fig. S1. DHP synthesis* by Horseradish peroxidase/H_2O_2 oxidation of coniferyl alcohol
*Note: In this experiment, aromatic carbons were all ^{13}C labelled.

Gel filtration chromatography (GFC)：
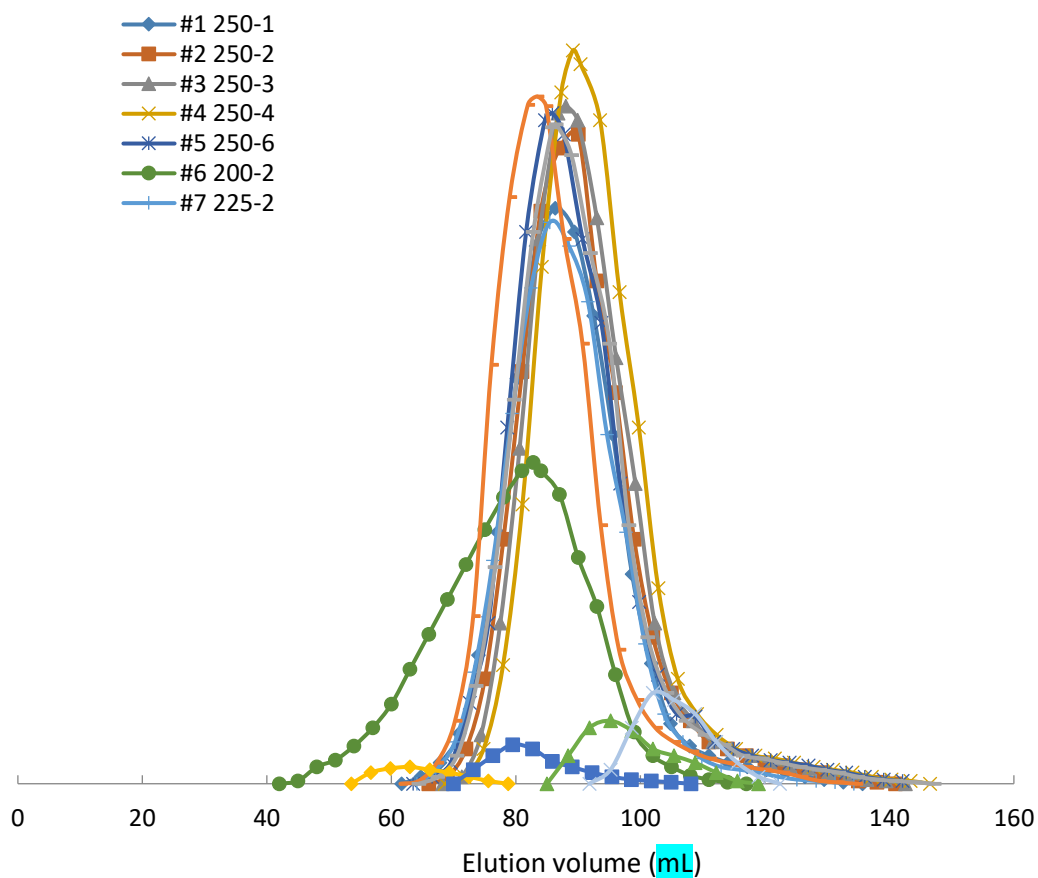
Fig. S2. Gel filtration curves of HSALs

Analysis of FT-IR spectra
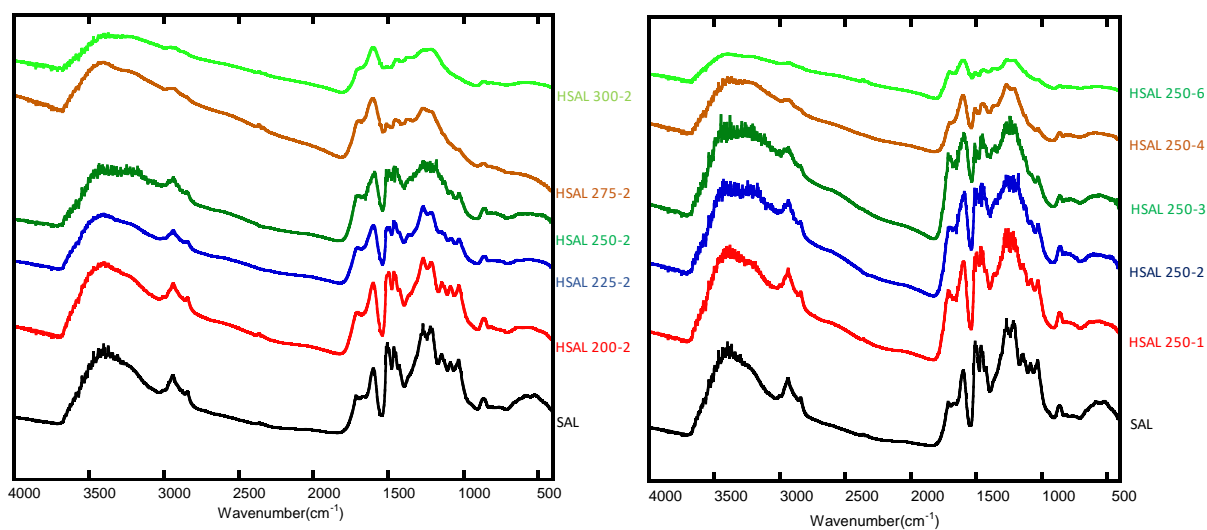
Fig. S3. FT-IR spectrum of SAL and HSALs

¹H/¹³C NMR spectra analysis of HSAL and kraft lignin
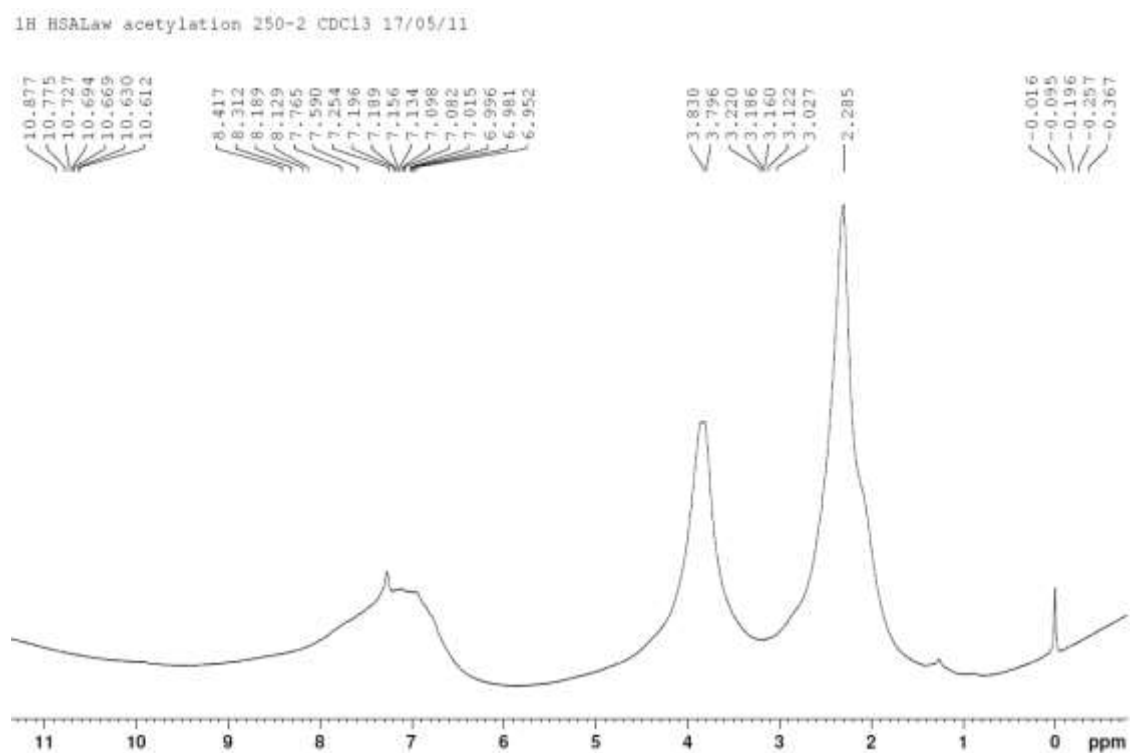
Fig. S4. ¹H NMR spectra analysis of acetylated HSALaw 250-2

13C HSALaw acetylation 250-2 CDCl3 #2 17/05/11

Fig. S5. ^{13}C NMR spectra analysis of acetylated HSALaw 250-2

HSAL show a high viscosity in liquid NMR organic solvents.

i) Dialyzed
ii) Freeze-dried

CDCl$_3$
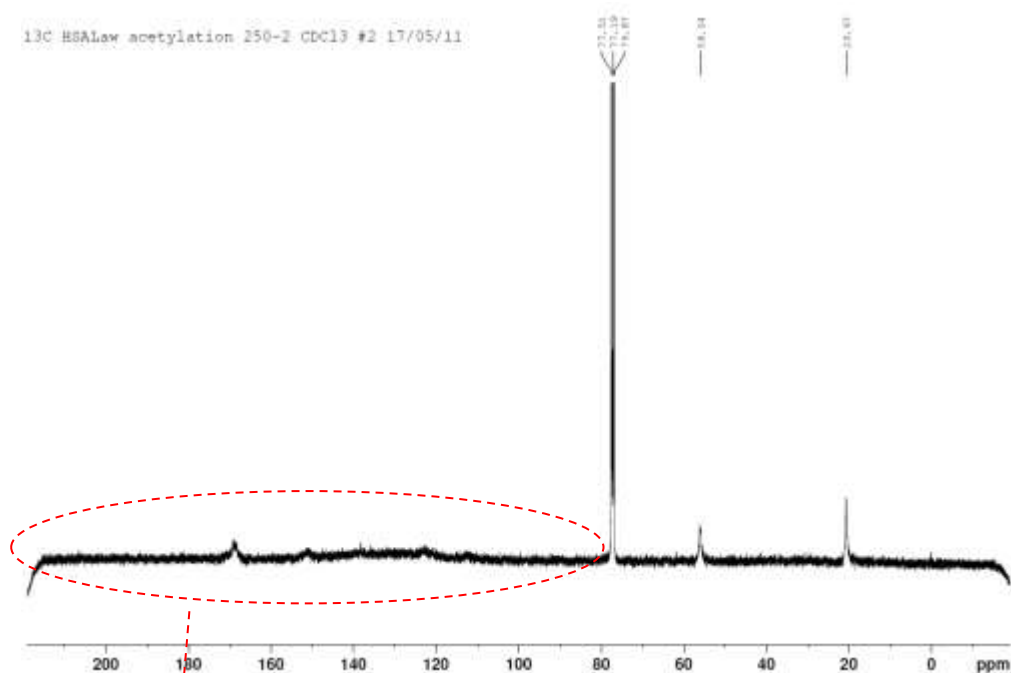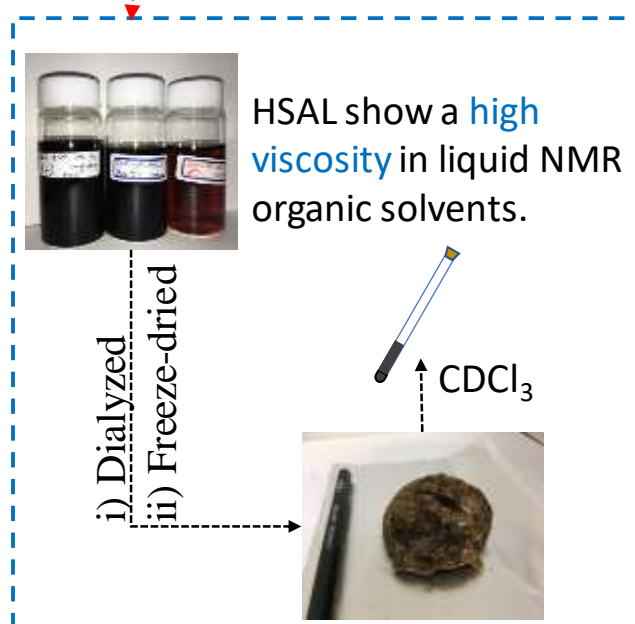
Note: As show above, HSAL show an unfriendly dissolution in NMR organic solvents (bright black and high viscosity), which cause a very low detection sensitivity on spectra by liquid-state NMR analysis.

bioresources.com

1H kraft-L N-aw acetylation   CDC13 17/05/14
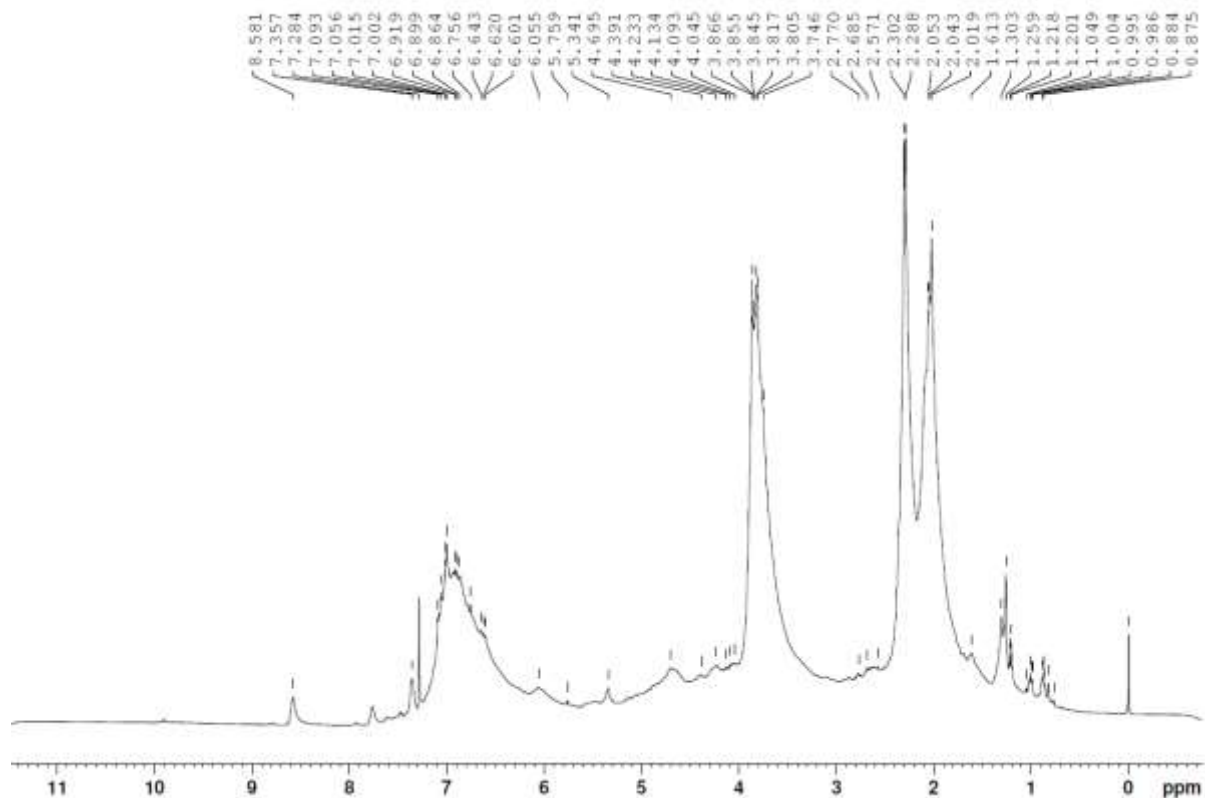
Fig. S6. ^{1}H NMR spectra analysis of acetylated kraft lignin

13C kraft-L N-aw acetylation   16000 CDC13 17/05/14
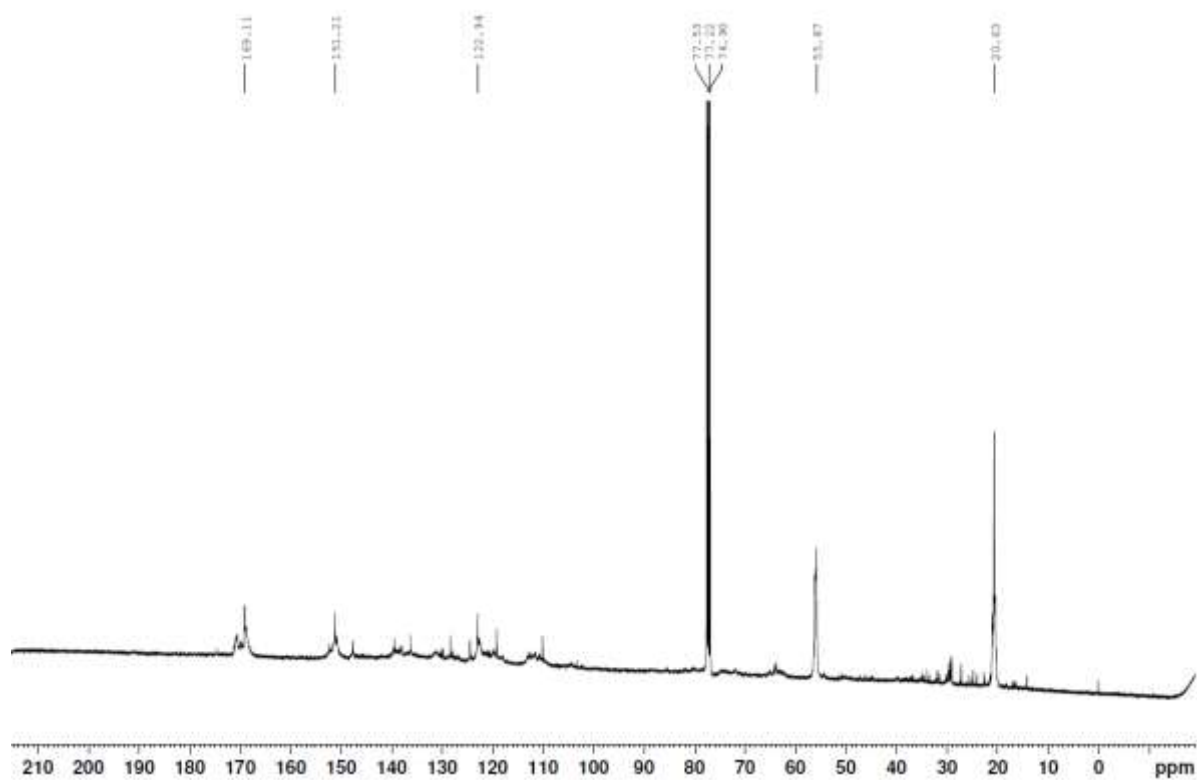
Fig. S7. ^{13}C NMR spectra analysis of acetylated kraft lignin

NMR Spectral Analysis of DHP

2D-HSQC NMR spectra analysis of ^{13}C labeled AHS-DHP is shown in Fig. 11. According to the database, its main structure was marked. Compared with unlabeled AHS-DHP, the signal strength of aromatic region was increased significantly. Based on those marked structure, a hypothesis of recondensation during hydrothermal treatment on DHP was carried out.
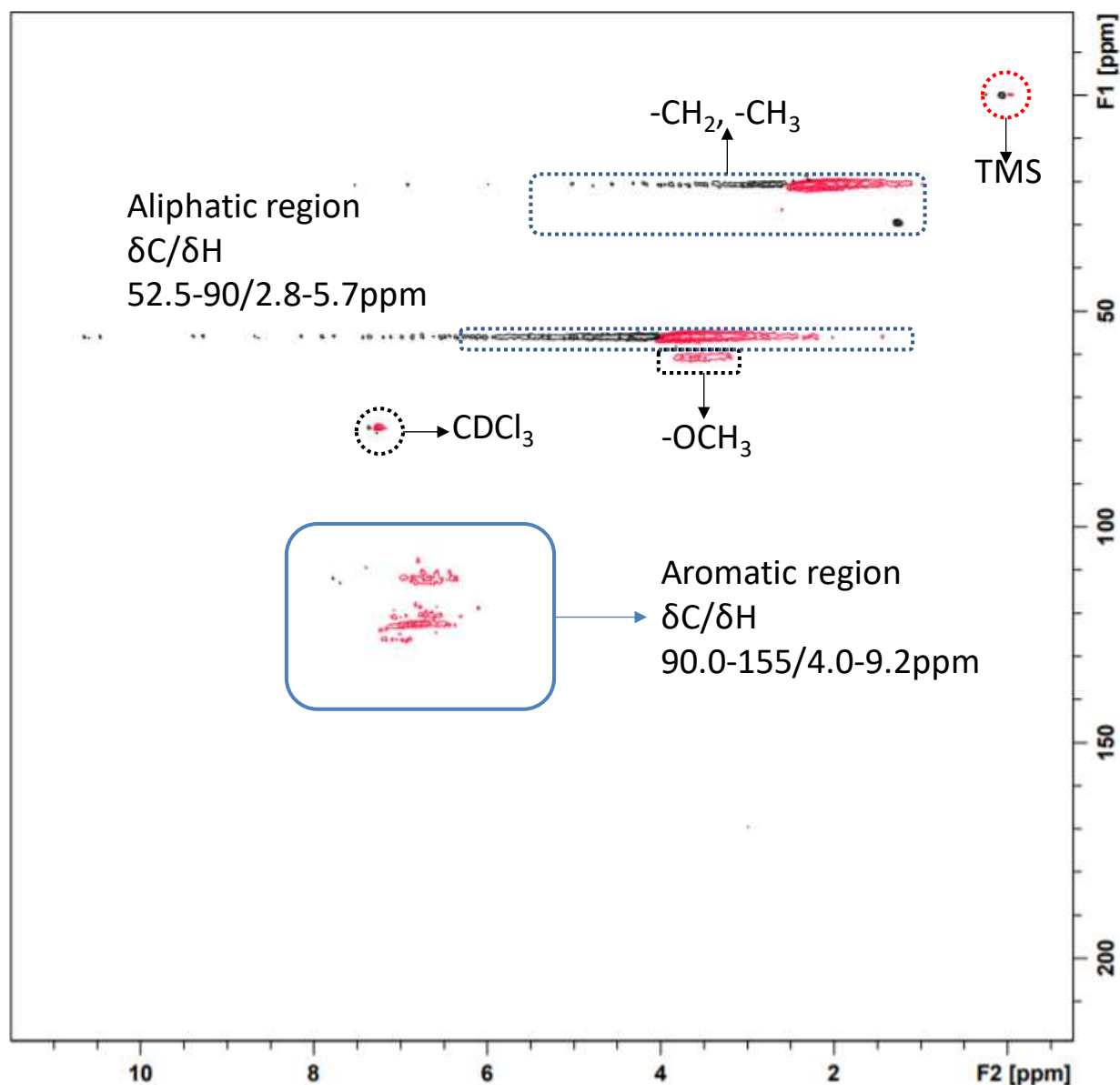
Fig. S8. 2D-HSQC NMR spectra analysis of AHS-DHP